

Nanoscale

Accepted Manuscript



This is an *Accepted Manuscript*, which has been through the Royal Society of Chemistry peer review process and has been accepted for publication.

Accepted Manuscripts are published online shortly after acceptance, before technical editing, formatting and proof reading. Using this free service, authors can make their results available to the community, in citable form, before we publish the edited article. We will replace this *Accepted Manuscript* with the edited and formatted *Advance Article* as soon as it is available.

You can find more information about *Accepted Manuscripts* in the [Information for Authors](#).

Please note that technical editing may introduce minor changes to the text and/or graphics, which may alter content. The journal's standard [Terms & Conditions](#) and the [Ethical guidelines](#) still apply. In no event shall the Royal Society of Chemistry be held responsible for any errors or omissions in this *Accepted Manuscript* or any consequences arising from the use of any information it contains.

Cite this: DOI: 10.1039/c0xx00000x

www.rsc.org/xxxxxx

ARTICLE TYPE

Rapid Formation of Ag_nX (X=S, Cl, PO₄, C₂O₄) Nanotubes via an Acid-Etching Anion Exchange Reaction

Jingjing Li,^a Wenlong Yang,^a Jiqiang Ning,^b Yijun Zhong,^{*c} and Yong Hu^{*a}

Received (in XXX, XXX) Xth XXXXXXXXX 20XX, Accepted Xth XXXXXXXXX 20XX

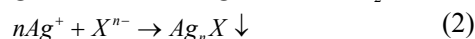
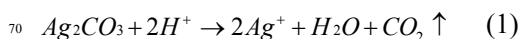
DOI: 10.1039/b000000x

This work presents a rapid nanotube fabrication method for a series of silver compounds Ag_nX, such as Ag₂S, AgCl, Ag₃PO₄, and Ag₂C₂O₄, from the pregrown Ag₂CO₃ nanorod templates. The involved anion exchange process takes place in non-aqueous solutions just at room temperature and completes within 10 minutes. An acid-etching anion exchange reaction mechanism has been proved underneath the transformation process from Ag₂CO₃ nanorods to Ag_nX nanotubes by the observation of intermediate yolk-shell nanostructure. It has been found that the final structure of the products can be conveniently controlled by simply varying the concentration of H_nX acids, and the employed organic solvents play a vital role in the formation of the nanotubes by effectively controlling the diffusion rates of different species of reacting ions. As a demonstration, the as-prepared AgCl and Ag₃PO₄ nanotubes exhibits enhanced photocatalytic activity and favorable recyclability for the photodegradation of rhodamine B (RhB) under visible-light irradiation.

One-dimensional (1D) tubular nanostructures, with distinct anisotropic features originating from higher geometrical aspect ratios, have received extensive research efforts due to their prospective applications in adsorbents, catalysis, drug delivery, microreactors.¹ Especially, the synthesis of 1D inorganic nanotubes (NTs) with tailored properties and desired applications is of both scientific and technological interest owing to the beneficial influence of dimensionality on electronic and optical properties.² In addition to the well-known carbon NTs, a variety of metal and semiconductor NTs have been synthesized by various methods, including self-rolling,³ Ostwald ripening,⁴ template-assisted method,⁵ ion exchange reaction,⁶ Kirkendall effect,⁷ and so on. These methods generally require high temperatures, special conditions, or template-removing procedures, which consequently limits their wide applications. Therefore, looking for low-cost, appropriate and mild method to fabricate inorganic NTs with uniform morphology and good structural stability remains a challenging but exciting topic in materials science.

Very recently, our group has successfully synthesized a series of metal sulfide-silver heterostructured NTs from Ag₂CO₃ nanorod templates via a microwave-assisted method.⁸ Herein, we demonstrate another facile generic strategy for preparing a series of Ag_nX (X= S, Cl, PO₄, C₂O₄) NTs from pregrown Ag₂CO₃ nanorods via a rapid acid-

etching anion exchange process in non-aqueous media at room temperature. This straightforward synthesis strategy is schematically depicted in Fig. 1, and the detailed experimental procedure is described in the ESI†. For this strategy, besides the use of organic solvents, the amount of acid is also a crucial parameter in determining for the formation of uniform Ag_nX NTs, which effectively controls the diffusion rates of hydrogen ion (H⁺) and acid radical ion (Xⁿ⁻) in the chemical transformation process. Owing to the lower solubility of Ag_nX relative to Ag₂CO₃, Ag₂CO₃ could adopt a thermodynamically favored direction to transform into Ag_nX by reacting with H_nX. Similar to the hard-template method, Ag₂CO₃ nanorod plays a role of sacrificial template which determines the product morphology. It is discovered that the organic solvents and the acid concentration are the determining factors to the successful acquisition of tubular structures. The involved chemical reactions for the formation of Ag_nX NTs can be described as follows:



Compared with a traditional double decomposition reaction, the whole chemical transformation process is controlled by two reaction steps. According to reaction (Eq. 1), Ag⁺ ions are released into the organic solution from Ag₂CO₃ nanorods which reacts with H⁺ ions. Particularly, Ag₂CO₃ is a solid reactant suspended in the organic solution, and the reaction takes place locally right in the very vicinity of the nanorods. As a result, the released Ag⁺ ions are localized to a close environment right surrounding the Ag₂CO₃ nanorods, and the local concentration of Ag⁺ ions is determined mainly by the initial concentration of H_nX and the diffusion rates of H⁺ ions towards the local region. Ag_nX is formed right in the local environment according to reaction (Eq. 2), and consequently precipitate onto the solid surface of the Ag₂CO₃ nanorods. As the reaction progresses, a shell of Ag_nX is produced on the Ag₂CO₃ core, forming intermediate Ag₂CO₃-Ag_nX yolk-shell nanostructures. After the formation of the Ag_nX shells, the diffusion conditions in the local environment get changes. Due to larger ionic radius of Xⁿ⁻ than that of hydrogen ion, the diffusion of Xⁿ⁻ across the Ag_nX shell is expected to be much slower than H⁺ ions. And it's even possible that Xⁿ⁻ ions can be blocked out of the shells. Since H⁺ ions can go across the shells, reaction (Eq.1) continues to take place and a higher concentration of Ag⁺ is created inside the Ag_nX shells. Reaction (Eq.2) therefore continues as the Ag⁺ ions diffuse out of the core region and more Ag_nX precipitate on

the shells, leading to continuous growth of the tubular structure. The above described process can be attributed to an acid-etching anion exchange reaction mechanism with non-equilibrium inter-diffusion process,⁹ through which the inner core materials evacuate outward continuously, finally generating a hollow interior. Besides, it should be noted that the whole chemical transformation process get completed very rapidly within 10 min, and just at room temperature. This acid-etching anion exchange reaction method appears as a simple and reproducible route for large-scale synthesis of uniform hollow structures.

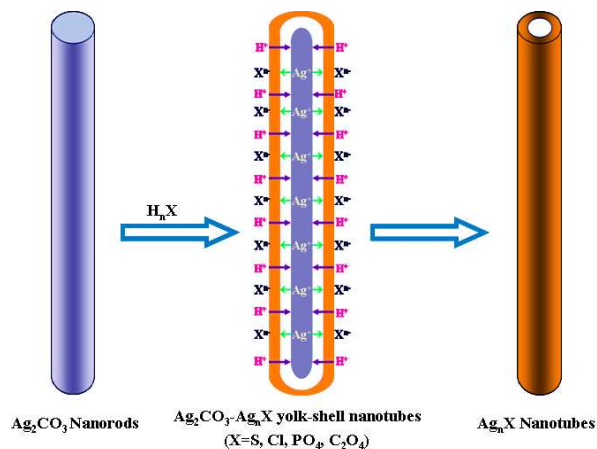


Fig. 1 Schematic illustration of the conversion processes from Ag_2CO_3 nanorods to Ag_nX nanotubes via an acid-etching anion exchange reaction.

X-ray powder diffraction (XRD) technique was used to examine the phase purity and crystallographic structure of the Ag_nX NT products. Fig. 2 depicts the XRD patterns recorded from four products which can be clearly indexed as primitive monoclinic structured Ag_2S (JCPDS card No.14-0072), face-centered cubic AgCl (JCPDS card No.31-1238), primitive cubic Ag_3PO_4 (JCPDS card No. 06-0505), and primitive monoclinic $\text{Ag}_2\text{C}_2\text{O}_4$ (JCPDS card No. 22-1335), respectively. These narrow and strong diffraction peaks of all the samples suggest that the Ag_nX products are highly crystallized. No Ag_2CO_3 diffraction signals or other additional peaks were detected from any of the XRD patterns, which indicate complete conversion of Ag_2CO_3 templates and high purity of all the products.

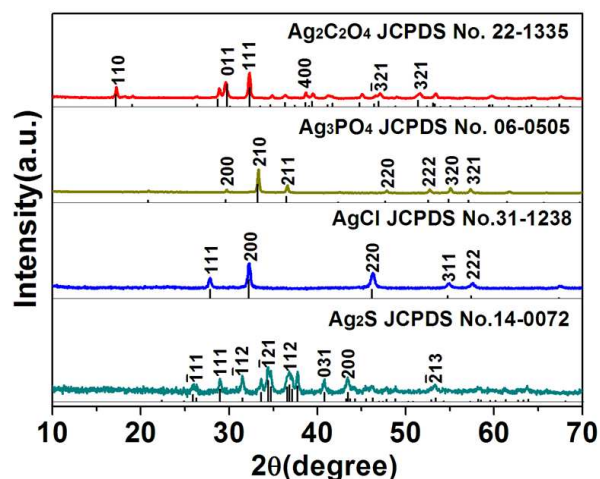


Fig.2 XRD patterns of the as-prepared Ag_nX ($X=\text{S}, \text{Cl}, \text{PO}_4, \text{C}_2\text{O}_4$) NTs.

Scanning electron microscopy (SEM) characterization was performed on all the products, and representative SEM images are shown in Fig. 3a-d. It can be clearly seen that all of the Ag_nX samples possess perfect and regular tubular structures about 200 nm in diameter and 2 μm in length, the bigger size than that of the Ag_2CO_3 nanorod precursors (see ESI†, Fig. S1). The structure details of the products were further examined with transmission electron microscopy (TEM) measurements. Fig. 3e shows a typical TEM image of the as-prepared Ag_2S NTs whose structure is in good agreement with the SEM observation. The high resolution TEM image of a closed bottom of NT and a section of NT wall is shown in Fig. 3f. It can be seen that wall thickness is about 10 nm, and the fringe interlayer spacing is about 0.25 nm, corresponding to the (112) crystal plane of primitive monoclinic Ag_2S . It is discovered that the organic solvents have a great effect on the final morphology of the Ag_nX NTs. When the synthesis is carried out in an aqueous solution, only anomalous morphologies including nanoparticles and nanorods are observed and no NTs are obtained (See ESI†, Fig. S2). This result can be explained by the lower diffusion rate of H^+ and X^{n-} in organic solvents due to their higher viscosity and lower polarity, which prohibits the rapid growth of Ag_nX into nanoparticles and nanorods. To obtain hollow nanostructures, we selected ethanol as the solvent to prepare Ag_2S and Ag_3PO_4 NTs and chose ethylene glycol (EG) as the solvent to obtain AgCl and $\text{Ag}_2\text{C}_2\text{O}_4$ NTs in this work. It is proved that the higher viscosity of EG decreases the diffusion rate of Cl^- and $\text{C}_2\text{O}_4^{2-}$ ions, and leads to the formation of perfect NTs (see ESI†, Fig. S3).

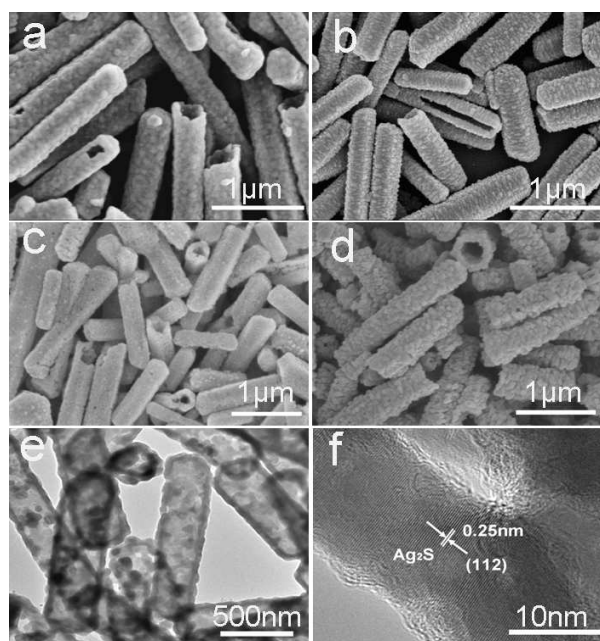


Fig. 3 SEM images of the as-prepared Ag_nX NTs: (a) Ag_2S ; (b) AgCl ; (c) Ag_3PO_4 ; (d) $\text{Ag}_2\text{C}_2\text{O}_4$; (e) TEM and (f) HRTEM images of Ag_2S NTs.

Structural analyses of partially transformed intermediate nanostructures provide important evidence for the growth mechanism of the obtained NT structures. By controlling the H_nX concentrations, we prepared a series of products for examination. From the XRD patterns (see ESI†, Fig. S4) of these products from the different amount of H_nX , obvious Ag_2CO_3 diffraction peaks are measured in addition

to the other peaks can be well assigned to different Ag_nX species, indicating co-existence of Ag_2CO_3 and Ag_nX in the intermediate products. SEM and TEM characterizations provide insights into the formation mechanism of Ag_nX NTs and the morphology and detailed structure of the as-prepared Ag_2CO_3 - Ag_nX yolk-shell NTs. We take the case of Ag_2S as an example, the transformation process of Ag_2CO_3 - Ag_2S nanostructures was tracked by adding different amounts of H_2S . In this synthesis, we employed a certain amount of thioacetamide (TAA) and a predetermined volume of CH_3COOH (20, 40, 60 μL) to produce different amounts of H_2S . Fig. 4 shows the representative SEM and TEM images of the intermediate products. These images reveal the evolution process of the surface morphology and the interior structure from the original nanorods to the final NTs. Firstly, thin layers of Ag_2S grow onto the Ag_2CO_3 template through the surface anion exchange reaction to form a Ag_2CO_3 - Ag_2S yolk-shell structure. With the increase of the acid amount, the interior of the solid rods gradually dissolved until the formation of fully converted Ag_2S NTs. The well-dispersed Ag_2S NTs were obtained with the CH_3COOH volume of 80 μL . The energy dispersive X-ray spectrometry (EDS) analysis also indicates that the Ag/S molar ratio in the yolk-shell nanocomposite decreases when the volume of CH_3COOH is increases, as shown in Table S1 (see ESI[†]). From the structural and composition analyses of partially and fully converted Ag_2S NTs, the acid-etching anion exchange reaction mechanism is further confirmed. To further investigate the function of acids in this reaction, a series of the corresponding salts, including Na_2S , NaCl , Na_2HPO_4 , and $\text{Na}_2\text{C}_2\text{O}_4$, are introduced into in the anion exchange reaction process, respectively. From the SEM images of the as-obtained Ag_nX products (Fig. S5, see ESI[†]), only some irregular nanorods can be observed.

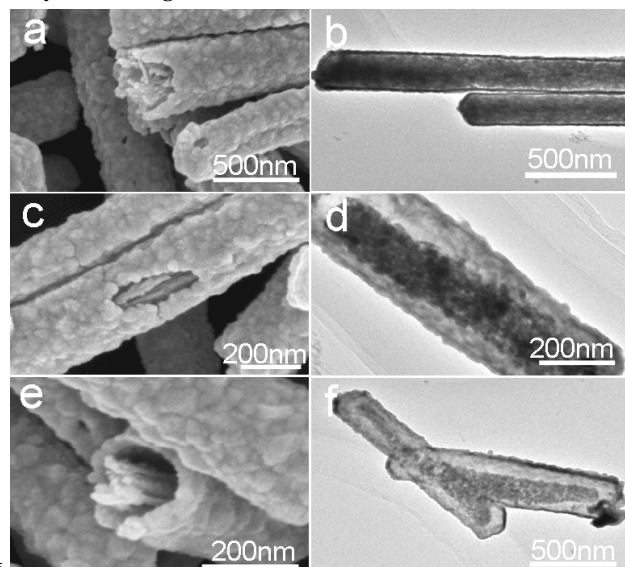
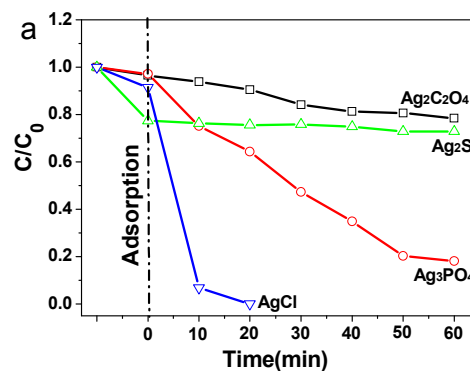


Fig. 4 SEM (left) and TEM (right) images of partially exchanged yolk-shell Ag_2CO_3 - Ag_2S nanostructures obtained with the different volumes of CH_3COOH : (a, b) 20 μL ; (c, d) 40 μL ; and (e, f) 60 μL .

Recent studies have suggested that hollow nanostructures might possess advantages, such as more surface active sites and better permeability, which is favorable for the special charge transfer and therefore superior photocatalytic performance.¹⁰ Additionally, 1D nanostructures exhibit significantly enhanced catalytic efficiency also due to high surface-to-volume ratio,

enhanced light scattering and absorption, rapid transport of free electron along the long axis and efficient electron-hole utilization.¹¹ Furthermore, various Ag-based compounds photocatalysts, such as AgCl , Ag_3PO_4 , have attracted much attention and have proved to be a new family of highly efficient visible-light-driven photocatalytic materials.¹² As a proof-of-concept demonstration of the functional properties of the as-prepared Ag_nX NTs, we carried out photocatalytic experiments in the present work. Fig. 5a presents the photocatalytic activities of the as-prepared Ag_nX NTs, which were evaluated for the degradation of organic dye rhodamine B (RhB) under visible-light irradiation, where C stand for the concentration of RhB after light irradiation for a certain period, and C_0 is the original concentration of the RhB. It can be seen that the as-prepared Ag_3PO_4 and AgCl NTs degrade RhB effectively, while $\text{Ag}_2\text{C}_2\text{O}_4$ and Ag_2S NTs display inconspicuous photocatalytic activities under the same conditions. Fig. 5b shows the stability and reusability of the AgCl photocatalyst by collected and reused the photocatalyst for six cycles. Because AgCl is unstable under visible-light irradiation, Ag nanoparticles are deposited on the surface of AgCl NTs during photocatalytic process. The XRD pattern of AgCl NT samples after six cycle photocatalytic test (see ESI[†], Fig. S6) indicates the existence of Ag. The stability of the Ag/ AgCl photocatalyst may be attributed to the fact that a photon is absorbed by the Ag nanoparticles, and an electron separated from an absorbed photon remains in the Ag nanoparticles rather than being transferred to the Ag^+ ions of the AgCl lattice under visible-light irradiation.¹³ In addition, 6 cycles of degradation of RhB using Ag_3PO_4 NTs as photocatalysts is shown in Fig. S7 (see ESI[†]).



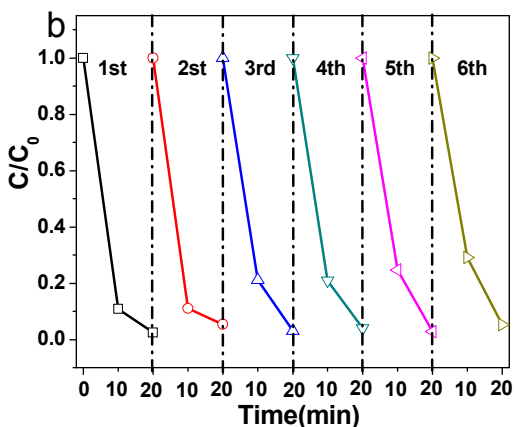


Fig. 5 (a) Photodegradation of RhB in the presence of different Ag_nX NTs under visible-light illumination. (b) 6 cycles of degradation of RhB using AgClNTs as the photocatalyst.

In summary, we have demonstrated a simple and reproducible strategy for the synthesis of a series of Ag_nX NTs with uniform morphology via an acid-etching anion exchange reaction at room temperature. Compared with those widely used solution methods, this route is a rapid, facile and more scalable synthesis of highly uniform NTs. As a proof-of-concept demonstration of the functional properties of these NTs, the as-prepared AgCl and Ag₃PO₄ NTs exhibit excellent photocatalytic activity and favorable recyclability for the degradation of organic dye under visible light radiation. It is believed that this new synthesis strategy is not restricted to the specific materials discussed in this work and can be extended to the preparation of a wide range of hollow nanostructures for different applications.

Acknowledgements

Financial support from the Natural Science Foundation of China (21171146) and Zhejiang Provincial Natural Science Foundation of China for Distinguished Young Scholars (LR14B010002) is gratefully acknowledged by Y. Hu.

Notes and references

^a Key Laboratory of the Ministry of Education for Advanced Catalysis Materials, Institute of Physical Chemistry, Zhejiang Normal University, Jinhua, 321004, P. R. China. E-mail: yonghu@zjnu.edu.cn

^b Department of Physics and HKU-CAS Joint Laboratory on New Materials, The University of Hong Kong, Pokfulam Road, Hong Kong, P.R. China.

^c College of Chemistry and Life Sciences, Zhejiang Normal University, Jinhua, 321004, P. R. China. E-mail: yjzhong@zjnu.cn

† Electronic Supplementary Information (ESI) available: [Detailed experimental procedures, additional SEM images, XRD pattern. See DOI: 10.1039/b000000x/]

- (a) C. B. Gao, Z. D. Lu and Y. D. Yin, *Langmuir* 2011, **27**, 12201; (b) D. K. Unruh, K. Gojdas, A. Libo and T. Z. Forbes, *J. Am. Chem. Soc.*, 2013, **135**, 7398; (c) R. Fan, Y. Y. Wu, D. Y. Li, M. Y. Yue, A. Majumdar and P. D. Yang, *J. Am. Chem. Soc.*, 2003, **125**, 5254.
- (a) C. N. R. Rao and A. Govindaraj, *Adv. Mater.*, 2009, **21**, 4208; (b) C. Bae, H. Yoo, S. Kim, K. Lee, J. Kim, M. M. Sung and H. Shin, *Chem. Mater.*, 2008, **20**, 756; (c) L. Cademartiri and G. A. Ozin, *Adv. Mater.*, 2009, **21**, 1013; (d) Y. N. Xia, P. D. Yang, Y. G. Sun, Y. Y. Wu, B. Mayers, B. Gates, Y. D. Yin, F. Kim and H. Q. Yan, *Adv. Mater.*,

2003, **15**, 353; (e) O. Carny, D. E. Shalev, E. Gazit, *Nano Lett.*, 2006, **6**, 1594.

- X. L. Lu, G. Q. Zhang, W. Wang and X. G. Li, *Angew. Chem. Int. Ed.*, 2007, **46**, 5772.
- S. Sakurai, H. Nishino, D. N. Futaba, S. Yasuda, T. Yamada, A. Maigne, Y. Matsuo, E. Nakamura, M. Yumura and K. Hata, *J. Am. Chem. Soc.* 2012, **134**, 2148.
- J. F. Ye, H. J. Zhang, R. Yang, X. G. Li and L. M. Qi, *Small* 2010, **6**, 296.
- S. F. Zhuo, Y. Xu, W. W. Zhao, J. Zhang and B. Zhang, *Angew. Chem. Int. Ed.*, 2013, **52**, 8602.
- (a) H. J. Fan, U. Gosele and M. Zacharias, *Small* 2007, **3**, 1660; (b) Y. Yang, R. B. Yang, H. J. Fan, R. Scholz, Z. P. Huang, A. Berger, Y. Qin, M. Knez and U. Gosele, *Angew. Chem. Int. Ed.*, 2010, **49**, 1442; (c) Q. Peng, X.-Y. Sun, J. C. Spagnola, C. Saquing, S. A. Khan, R. J. Spontak and G. N. Parsons, *ACS. Nano.*, 2009, **3**, 546; (d) Y. D. Yin, R. M. Rioux, C. K. Erdonmez, S. Hughes, G. A. Somorjai and A. P. Alivisatos, *Science.*, 2004, **304**, 711.
- (a) Y. R. Wang, W. L. Yang, L. Zhang, Y. Hu and X. W. Lou, *Nanoscale*, 2013, **5**, 10864; (b) W. L. Yang, L. Zhang, Y. Hu, Y. J. Zhong, H. B. Wu and X. W. Lou, *Angew. Chem. Int. Ed.*, 2012, **51**, 11501.
- H. J. Fan, M. Knez, R. Scholz, K. Nielsch, E. Pippel, D. Hesse, M. Zacharias and U. Gosele, *Nat. Mater.*, 2006, **5**, 627.
- (a) W. L. Yang, Y. Liu, Y. Hu, M. J. Zhou and H. S. Qian, *J. Mater. Chem.*, 2012, **22**, 13895; (b) Y. Liu, L. Yu, Y. Hu, C. F. Guo, F. M. Zhang and X. W. Lou, *Nanoscale*, 2012, **4**, 183; (b) S. L. Wang, H. H. Qian, Y. Hu, W. Dai, Y. J. Zhong, J. F. Chen and X. Hu, *Dalton Trans.*, 2013, **42**, 1122; (c) H. F. Cheng, B. B. Huang, Y. Y. Liu, Z. Y. Wang, X. Y. Qin, X. Y. Zhang and Y. Dai, *Chem. Commun.*, 2012, **48**, 9729.
- Y. Liu, L. Zhou, Y. Hu, C. F. Guo, H. S. Qian, F. M. Zhang and X. W. Lou, *J. Mater. Chem.*, 2011, **21**, 18359.
- (a) Y. P. Bi, S. X. Ouyang, N. Umezawa, J. Y. Cao and J. H. Ye, *J. Am. Chem. Soc.*, 2011, **133**, 6490; (b) Y. P. Bi, S. X. Ouyang, J. Y. Cao and J. H. Ye, *Phys. Chem. Chem. Phys.*, 2011, **13**, 10071.
- P. Wang, B. B. Huang, X. Y. Qin, X. Y. Zhang, Y. Dai, J. Y. Wei and M. H. Whangbo, *Angew. Chem. Int. Ed.* 2008, **47**, 7931.